Distribution and Steepness of Ripples on Carrier Waves

JIN WU

College of Marine Studies, University of Delaware, Newark, DE 19711

(Manuscript received 28 December 1978, in final form 19 March 1979)

ABSTRACT

The slopes of ripples and the profiles of their carrier waves were simultaneously measured in a wind-wave tank with winds of various velocities blowing over preexisting, long, regular surface waves. The results include the apportionment and the slope distributions (and therefore the mean-square slopes) of ripples located on various portions of the carrier-wave profile. At low wind velocities, the surface-tension governing regime of wind-wave interaction, the leeward face of the carrier wave was found to contain more ripples than the windward face. The parasitic capillaries are concentrated on the upper half of the leeward face, and move along the leeward face toward the trough of carrier waves as the wind velocity increases. At high wind velocities, the gravity governing regime of wind-wave interaction, the ripples become more evenly distributed on the leeward and on the windward faces. However, the ripples on the windward face are concentrated near the carrier-wave crest, and the ripples on the leeward face are concentrated near the carrier-wave trough. At all wind velocities, the rms slope of ripples on the windward face of the carrier waves is greater than that on the leeward face.

1. Introduction

Many measurements (Schooley, 1954; Cox and Munk, 1956; Cox, 1958; Wu, 1971; Keller and Wright, 1975; Long and Huang, 1976; and Wu 1977a) have been conducted to determine the gross statistics of microstructures of wind-generated waves. Some of the investigators also attempted to study the distribution of ripples along the profile of long waves; however, they made only oblique observations and never obtained the actual distribution. A technique of selective sampling was used by Wu (1973) and Lee (1977) to determine such a distribution, which is helpful not only in understanding nonlinear energy transfers from wind to waves (Longuet-Higgins, 1969; Hasselmann, 1971; Wu, 1972) and among wave components (Longuet-Higgins, 1963; Phillips, 1963) but also in setting viewing angles of microwave sensors over the sea surface and interpreting results of oceanic microwave measurements (Jones *et al.*, 1977). Doppler measurements with radar were performed by Lee (1977) at a low wind velocity and small wave steepnesses, while an optical instrument was used by Wu (1973) under a wide range of wind velocities and large wave steepnesses, to study the correlation between wind-generated ripples and long gravity waves. The previously unpublished data of the latter study are analyzed; the results include the distribution and the slope statistics of ripples on various segments of carrier-wave profiles.

The present study generally supports the conclusions drawn by others from observations on the roughening of carrier-wave profiles at low wind velocities, and suggests that these conclusions must be modified at high wind velocities. The present results also include, for the first time, the steepnesses of ripples on various segments of carrier-wave profiles, indicating that the steepness (the rms slope) of ripples does not always correspond to the number of ripples located on the carrier-wave profile. While it is generally true that more ripples are located on the leeward than on the windward face of the carrier waves, the rms slope of ripples on the windward face is found to be actually greater than that of ripples on the leeward face. The results are discussed in terms of the application in remote sensing and the understanding of wave dynamics.

2. Experiments

a. Equipment, instruments and experimental conditions

The experiments were conducted in a tank 1.5 m wide and 22 m long. An axial fan was mounted at the upwind end of the tank, which was covered for the first 15 m to provide a wind tunnel 0.31 m high above water 1.24 m deep. The test section was located at the middle length of the tank. The airflow boundary layer in the tank became aerodynamically rough at a wind velocity of 2.5 m s^{-1}. The tank was also equipped with a mechanical, flap-type wave generator. The present study was conducted with winds of four different velocities blowing over pre-

0022-3670/79/051014-08$06.00

existing mechanically generated waves with a height of 4.5 cm and a length of 1 m. The friction velocities of the wind, determined from the logarithmic velocity profiles, are shown in Table 1.

Two simultaneous wave measurements were made: a conductivity probe for recording (long) carrier-wave profiles and an optical instrument for measuring (short) ripple slopes. The conductivity probe consisted of a vertically suspended and partially submerged platinum wire 0.13 mm in diameter. The optical instrument, supported over the tank, consisted principally of a light source and a light sensor. The central axis of a radial instrument plane, containing the light sheet from the light source and the axis of the light sensor, was at the mean water surface and perpendicular to the wind direction. This radial plane could be set at any desired inclination from the mean water surface. The sensor received the light reflected by the water surface only when the portion of water surface viewed by the sensor (0.7 mm in diameter) was normal to the instrument plane. The short side of the light sheet was aligned with the direction of wind to make the instrument insensitive to the crosswind slope. The angular resolution of the instrument to the water surface slope in the wind direction was about 1°. Any wave with its length greater than the diameter of the sensing spot on the water surface (0.7 mm) and with the slope change from one face to the other exceeding the angular resolution (1°) can be detected by the present instrument. During the experiment, the instrument was set successively at various inclinations to measure the occurrence of the corresponding upwind-downwind slopes of the disturbed water surface. The signals of the optical instrument are light pulses, each pulse representing the occurrence of the designated surface slope, and the pulse width is the time required for a detectable water surface slope to pass the instrument. A detailed description of the optical instrument has been reported elsewhere (Wu *et al.*, 1969). The conductivity probe and the focal spot of the optical instrument at the water surface longitudinally were within the same cross section of the tank, and transversely were at an equal distance (5 mm) from, but on different sides of, the middle tank width. The outputs of the conductivity probe and of the optical instrument were simultaneously recorded on separate channels of a tape recorder.

Since the wind-induced drift is known to modify the propagation (the dispersion relationship) of surface waves, additional experiments were conducted to measure the length of carrier waves, which were nearly regular in the present experiment. Two conductivity probes were used during this part of the experiment: the upwind probe was fixed and the downwind probe was supported on a sliding scale.

TABLE 1. Wind and wave conditions in present experiments.

Wind velocity U (m s^{-1})	4.18	6.92	9.60	12.25
Wind friction velocity u_* (cm s^{-1})	22.1	29.7	66.8	106.8
Wave height h (cm)	5.0	6.5	8.6	10.6
Wavelength λ (cm)	122	127	130	137
Wave steepness ka	0.129	0.161	0.208	0.243

The distance between probes was adjusted to make the wave signals from two probes, monitored on the scope, oscillate in phase; this distance is therefore the wavelength. The lengths (λ), the heights (h), and the steepnesses (ka, $k = 2\pi/\lambda$ and $a = h/2$) of carrier waves under four different wind velocities are shown in Table 1, in which U is the wind velocity measured at two-thirds of the tunnel height above the mean water surface. The height and length of preexisting waves were so chosen that the dominant (carrier) waves remained regular at all four wind velocities and with their regularity on the verge to be disturbed by wave breaking at the highest wind velocity.

b. Ripples and carrier waves correlation measurements

The carrier-wave profile was divided into different regions. A gating device was designed to separate and collect the light signals from the desired region. During the operation, the tape was played back at one quarter of the recording (real) speed,[1] with the carrier-wave profile monitored on the oscilloscope and with the simultaneously recorded light signals passing through the gating device. The switch of the gate was controlled by an operator who watched the monitored trace of carrier waves. The gating device was operated so as to feed only light pulses produced by ripples located on the designated portion of the carrier-wave profile to a pulse accumulator, where the period of the pulse is accumulated. More on the data analysis will be discussed in the next section.

The use of mechanically generated, long, regular waves is necessary for the correlation study. Otherwise, it would be very difficult to apply the gating technique to short, irregular dominant waves produced in the present tank. With wind blowing over preexisting waves, on the other hand, the carrier waves as discussed earlier remained regular and the undulation of the water surface could be easily traced by the operator. In other words, the preexisting waves served in the present experiment as a regulator for the correlation measurements.

[1] The tape was also played back at 1/16 of the recording speed with insignificantly different results.

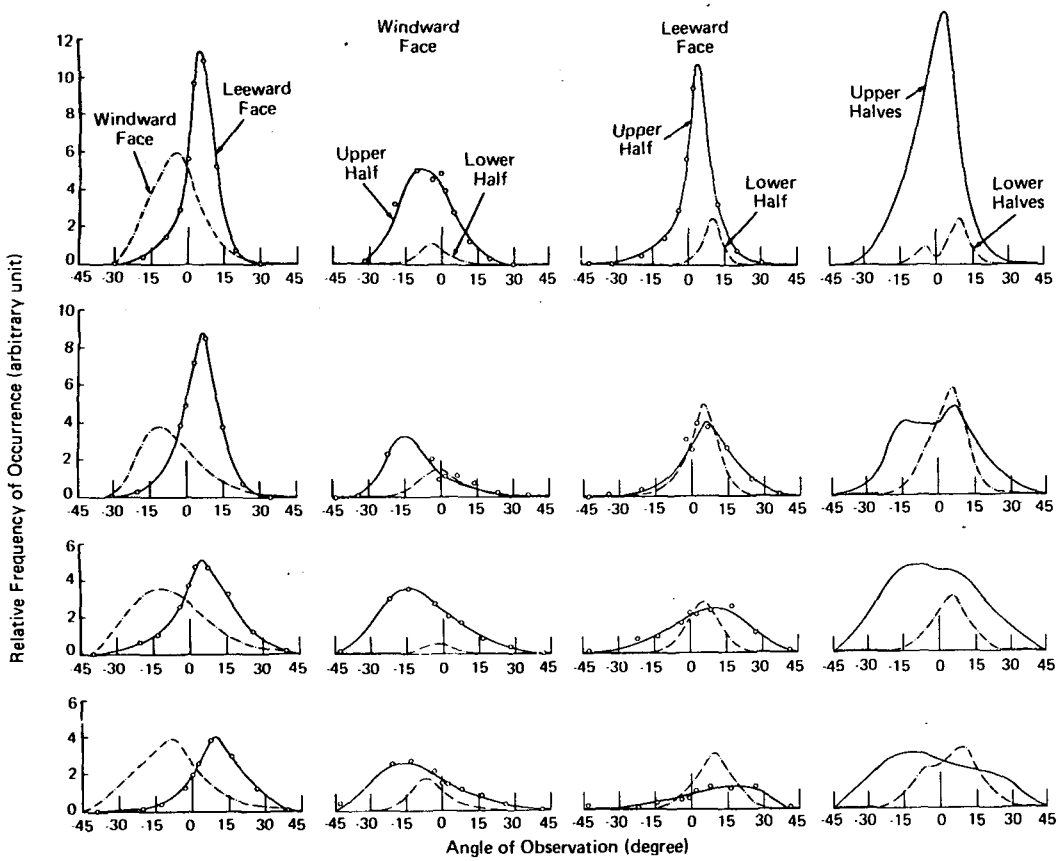

FIG. 1. Distribution of ripples along profiles of carrier waves. The results from top to bottom rows are obtained at U = 4.18, 6.92, 9.60 and 12.25 m s^{-1}, respectively.

3. Results

As discussed earlier, during the test with given wind and wave conditions the optical instrument was set successively at various angles of observation to detect the corresponding water-surface slopes. The temporal frequencies of occurrence of these slopes of the roughened water surface locating instantaneously on different segments of the carrier-wave profile were separately obtained while the tape was repeatedly played back. The slope distributions of ripples riding on the following portions of the carrier-wave profile were obtained directly from the tape: entire profile, leeward face, upper half of leeward face, and upper half of windward face. From these data, the slope distributions were deduced of ripples riding on the other portions of the carrier-wave profile: windward face, lower half of leeward face, lower half of windward face, upper halves (of both faces) near crest, and lower halves (of both faces) near trough.

a. Slope distributions of ripples on various carrier-wave segments

The slope distributions obtained at four different wind velocities are shown in Fig. 1; one row for each wind velocity and one column for the same two contrasting portions of the carrier-wave profile. The positive angle shown in the figure corresponds to a leeward slope (the optical instrument looking upwind) and the negative angle to a windward slope (the instrument looking downwind). Each data point shown in Fig. 1 was obtained from a 1 min run of the experiment (with the passing of 60–70 carrier waves), and a smooth curve was fitted by eye to the data. The slope distributions for the other sets are deduced from the fitted curves.

In a separate study, the slope distributions described by probability densities of either temporal frequencies or simply frequencies of occurrence were measured. The former took into account the pulse period, while the latter counted the occurrence of the light pulse regardless of its period. It was found that the slope distributions determined with both descriptions differed insignificantly except at low wind velocities in the surface-tension governing wind-wave interaction regime featuring parasitic capillaries. Even in this case, the slope distributions for both descriptions were still very similar; only the peak of the distribution occurred at a different slope. In summary, despite that the slope distributions shown in Fig. 1 are described by temporal

frequencies of occurrence, the maximum frequency of occurrence of the slope is still produced by crests and troughs of ripples. These crests and troughs are tilted by carrier waves, and therefore no longer have a zero slope. Consequently, the slope distribution of ripples riding on the leeward face of carrier waves is seen in Fig. 1 to peak at a positive angle, and that of ripples riding on the windward face to peak at a negative angle. The deviation of the peak from zero slope is therefore about the same as the average local slope of the carrier-wave profile. The distributions obtained from a single face of carrier waves are seen skewed in Fig. 1; double peaks are also seen in some of the distributions for upper and lower halves of both faces.

b. Distributions of ripples on various carrier-wave segments

As discussed above, the maximum frequency of occurrence of the water-surface slope, or the peak of the slope-distribution curve, is produced by the crests and troughs of ripples. For each wind velocity, the maximum frequency of occurrence is proportional to the number of ripples. Composite pictures showing relative distributions of ripples on various segments of the carrier-wave profile at different wind velocities are presented in Fig. 2. The four numbers indicated along the wave profile are the probability densities of occurrence of ripples riding on four respective segments of the carrier-wave profile. The numbers on top of the profile are the relative probabilities of occurrence for the windward and leeward faces, and the numbers on the right margin of Fig. 2 are those for the upper and lower halves of the profile. At high wind velocities (U = 9.60, 12.25 m s^{-1}), the carrier-wave profile became appreciably skewed with a shorter leeward face and a longer windward face; the numbers in parentheses are the values weighted to take into consideration the skewness of carrier-wave profile.

The ripples are seen to concentrate on the upper half of the leeward face of the carrier-wave profile at the lowest wind velocity, and become more evenly distributed on the leeward face as the wind velocity increases. Except at the highest wind velocity, more ripples are on the leeward than on the windward face, and again become more evenly distributed over both faces as the wind velocity increases. Among four segments, the lower half of the leeward face contains the most densely distributed ripples except at the lowest wind velocity; the lower half of the windward face contains the least densely distributed ripples for all wind velocities.

c. Root-mean-square surface slopes for various carrier-wave segments

The slope distributions of ripples riding on various segments of the carrier-wave profiles under different

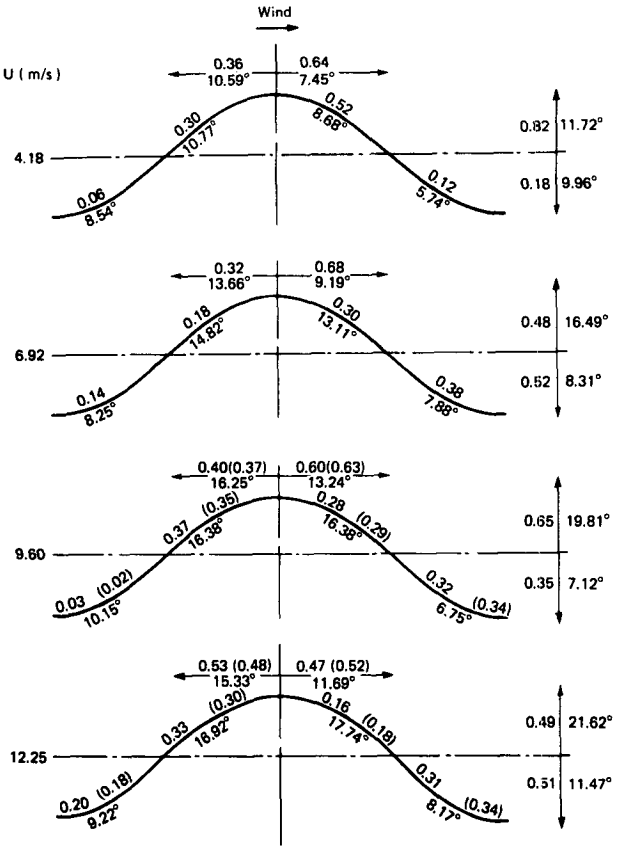

FIG. 2. Probability-density distributions and rms slopes (deg) of ripples along carrier-wave profiles. The wind direction is from left to right of the figure. The carrier-wave profile is divided by wave crest and trough and mean water surface into four segments, upper and lower halves of the windward face and upper and lower halves of the leeward face.

wind velocities are shown in Fig. 1. The rms slope is generally calculated with respect to the horizontal, mean water surface. However, the slopes of ripples on different segments of the carrier-wave profile are modulated by the local tilting of the water surface. Consequently, a true rms slope of ripples should be determined with respect to the slope of the tilted surface. As discussed previously, the tilting of each segment of the carrier-wave profile is related to the angle at which the maximum frequency of occurrence of slope for that particular segment takes place. In Table 2, the rms slopes were calculated from the individual slope distribution shown in Fig. 1 with respect to (a) zero slope, (b) mean slope, and (c) slope with the maximum frequency of occurrence of the respective distribution. In most cases the rms slopes calculated from (b) and (c) are nearly the same, and differ considerably from those calculated from (a). The results calculated with (a) are for reference only. The rms slopes calculated from (c) are believed to be the most reasonable representation; more confidence in using this group of results is gained from, as stated above, the closeness of the

TABLE 2. Root-mean-square slope. The slope is expressed in degrees; (a), (b) and (c) correspond to the three different calculations.

	Wind velocity U (m s^{-1})											
	4.18			6.92			9.60			12.25		
Segment of wave profile	(a)	(b)	(c)	(a)	(b)	(c)	(a)	(b)	(c)	(a)	(b)	(c)
Entire profile	7.72			9.99			11.88			12.92		
Leeward face	8.68	7.46	7.45	10.49	9.15	9.19	14.63	13.18	13.24	15.68	11.68	11.69
Windward face	11.80	10.60	10.59	13.91	12.72	13.66	17.23	15.42	16.25	17.46	15.35	15.33
Upper half—near crests	10.60	10.64	11.72	14.91	14.89	16.49	17.63	17.53	19.81	19.77	19.52	21.62
Lower half—near troughs	11.01	9.35	9.96	8.57	7.87	8.31	8.39	7.07	7.12	11.44	10.73	11.47
Leeward face												
Upper half	9.31	8.61	8.68	14.13	13.11	13.11	17.11	16.12	16.38	19.20	15.38	17.74
Lower half	10.95	5.69	5.74	8.45	7.73	7.88	8.61	6.75	6.75	12.15	8.17	8.17
Windward face												
Upper half	12.22	10.67	10.77	15.99	13.66	14.82	17.42	15.67	16.38	19.23	16.53	16.92
Lower half	9.12	8.49	8.54	8.16	8.17	8.25	10.15	10.09	10.15	9.94	9.07	9.22

values calculated from (b) and (c). The rms slopes calculated from (c) for various segments of the carrier-wave profile are also shown in degrees in Fig. 2.

It is clearly illustrated that, including parasitic capillaries featured at the lowest wind velocity, the rms slope of ripples on the windward face is greater than that on the leeward face. The slope of ripples on the upper portion of the carrier-wave profile is much steeper than on the lower portion; this is true for the whole profile as well as for the windward and leeward faces alone. Among the four segments, the ripples on the lower half of the leeward face are the least in steepness.

4. Comparison with other results

a. Upwind and downwind looks

The distribution and steepness of ripples along carrier waves are of great interest in the understanding of wave dynamics and the application of remote sensing. However, only oblique measurements of the microscopic structures of wind waves in laboratories were conducted by Wu (1971), Keller and Wright (1975) and Long and Huang (1976) by directing their sensors either upwind or downwind. The results obtained from upwind observations[2] were then considered by them to be more closely related to ripples on the leeward face of the carrier waves, while those from the downwind observations[2] were considered to be more closely related to the windward face. Along the same line, the upwind and downwind sea returns of radar were considered to have more contributions from the roughnesses of the leeward and windward faces of long waves, respectively (Jones *et al.*, 1977). It is of course realized by all investigators that oblique measurement samples ripples from the entire carrier-wave profile. In any event, inasmuch as none of the previous investigations reported similar measurements as in the present study, only qualitative comparison can be made between the present and their results.

The modulation in backscattered power from wind-generated ripples ($\lambda = 2.3$ cm) over pre-existing long waves ($h = 5.5$ cm, $\lambda = 2.9$ m) was measured in a wave tank by Keller and Wright (1975). The returns were obtained at various wind conditions with their sensor looking both upwind and downwind. Their measurement included both the hydrodynamic effects and the electromagnetic effects due to the tilting of the water surface (the slope of carrier waves), while the present measurements include the former and exclude the latter effects. These are the other reasons making direct and quantitative comparison difficult.

The results of Keller and Wright presented in terms of the fractional modulation from either upwind or downwind looks versus the wind-friction velocity, are reproduced in Fig. 3a. Much has been said by the authors for the portion of their results with $u_* < 40$ cm s^{-1}, where the modulation looking downwind is very small in comparison with that looking upwind. However, the trend is seen in Fig. 3a reversed for $u_* > 40$ cm s^{-1}, although not much attention has been paid by the authors to this reversal. Unlike Keller and Wright's technique, the optical measurements of short waves are not spectrally resolved; nonetheless, the present results shown in Fig. 2 appear to support this trend reversal. The upper half of the leeward face (related to the upwind look) contains many more ripples than the upper half of the windward face (related to the downwind look) for the top two profiles in Fig. 2 with $u_* < 40$ cm s^{-1}, and the trend is reversed for the bottom two profiles with $u_* > 40$ cm s^{-1}. In

[2] These observations are hereinafter referred to as "looks."

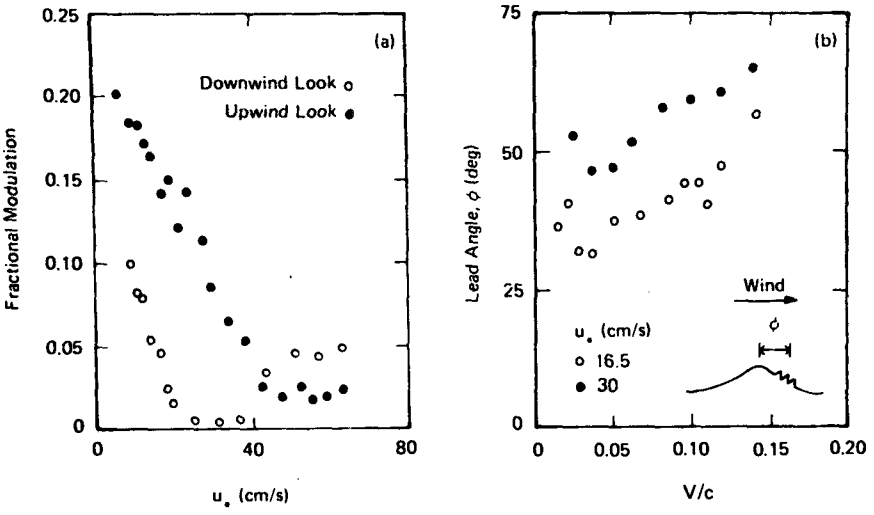

FIG. 3. Results of microwave scattering in a laboratory tank obtained by Keller and Wright (1975). Here $u*$ is the wind-friction velocity, c the phase velocity of plunger-generated waves, and V the modulus of the horizontal component of orbital velocity of plunger-generated waves.

other words, the trend of the data at high winds shown in Fig. 3a is supported by the present results, and is very much different from that at low winds.

In another series of measurements, Keller and Wright determined the phase angle ϕ by which the modulated microwave returns led the wave crest under two low wind velocities ($u*$ = 16.5 and 30 cm s^{-1}) and at various wave conditions. The wave condition is expressed in terms of the ratio between the modulus of horizontal component of orbital velocity V and the phase velocity c of plunger-generated waves. Their results, reproduced in Fig. 3b, clearly illustrate that the lead angle ϕ is greater at a higher wind velocity. This series of results are again in agreement with the top two profiles shown in Fig. 2 and discussed previously: as the wind velocity increases, the ripples move down the leeward face. It should be pointed out, however, that this is true only in the surface-tension governing regime of wind-wave interaction at low wind velocities.

The microwave radar responds to the energy of ripples related to both number of ripples per unit water surface area and steepness of ripples. The present results appear to indicate that radar returns are apparently more influenced by the roughnesses near the crests of long waves than by those near the troughs. It also appears that the returns are related more closely to the number (density) of ripples shown in Fig. 2 than to the steepness (rms slope) of ripples shown in Table 2 and Fig. 2.

b. Conditional sampling

The technique of conditional sampling was employed by Lee (1977) to determine the microwave signal returns from various portions of the gravity waves. He chose the following sampling locations denoted by the phase angle: forward node (0°), crest (90°), backward node (180°) and trough (270°). The band width was generally about ±45°, and sometimes up to ±60°. His experiments were conducted with wind waves superimposed on the mechanically generated long waves with a length of 30.8 cm and with various amplitudes under a wind velocity of 3.93 m s^{-1}; the steepness of the waves ranges from 0.024 to 0.112. His results indicated that the Doppler spectrum of the ripples peaked near 90° but on the leeward face for all steepnesses and insignificant returns from the trough.

It is clear that Lee's experiments, performed at a low wind velocity, were in the surface-tension governing regime of wind-wave interaction featuring the existence of parasitic capillaries. The present results at the lowest wind velocity (4.18 m s^{-1}) were obtained under experimental conditions comparable with Lee's. These results are shown in the upper right corner of Fig. 1 and the top profile of Fig. 2, illustrating that excessive number of capillaries are located on the upper half of the leeward face and near the carrier-wave crest. This phenomenon, however, can be visually observed and clearly photographed even without the assistance of the microwave sensor and the conditional sampling; with such an assistance, the observation of ripples of a given frequency can be made. The additional information provided by the present measurement is the slope statistics of these capillaries, as the radar returns are contributed by both the number of ripples per unit water surface area and their steepness. In addition, the present results also provide the reduction of the steepness of these capillaries as they move down the leeward face of the carrier-wave profile at a higher wind

velocity (6.92 m s^{-1}) in the same wind-wave interaction regime.

At high wind velocities in the gravity-governing regime of wind-wave interaction, it is impossible to describe the distribution of ripples on the basis of visual observations. It is into this velocity region that extension of observations made at low wind velocities is erroneous. The results shown in Fig. 1 obtained at higher wind velocities clearly do not follow the trend of the data obtained at the lowest wind velocity. In summary, Lee's results should be interpreted with caution, because his experiments were performed at a low wind velocity, and also at low wave steepnesses in comparison with the wave steepness in the present experiment shown in Table 1. It is more interesting for oceanographic applications to study the effects of nearly saturated gravity waves on wind-generated ripples.

5. Discussion

a. Upper halves versus lower halves—changes in the form of short waves on long waves

With the concept of radiation stress, Longuet-Higgins and Stewart (1960) have shown that short gravity waves, superimposed on much longer waves, have a tendency to become shorter and steeper at the crests of longer waves, and correspondingly longer and flatter in the troughs of the longer waves. No wind-wave interaction was considered by them. In other words, because of the radiation stress alone, the rms slope of ripples on the upper halves of their carrier-wave profiles should be greater than on the lower halves. The present results shown in Table 2 and Fig. 2 are clearly in support of this mechanism. Except at the lowest wind velocity where parasitic capillaries are featured, the rms slope of the upper halves is about, or even more than, twice that of the lower halves, representing the greatest difference between any contrasting portions of the carrier-wave profile.

The effects of gravity waves on the ripples described above were also observed by Lee (1977) at a low wind velocity with much greater radar returns from the crests than from the troughs of the gravity waves. However, as discussed previously, he was not able to distinguish whether the greater returns are due to more ripples or the steepening of ripples. Comparing the distribution of ripples and the rms slopes shown in Fig. 2, we see that more ripples are not necessarily accompanied by a greater rms slope; only the latter indicates the ripple steepening. Therefore, the present results provide clearer evidence on the steepening of ripples near the crests and the flattening near the troughs of long waves.

b. Windward face versus leeward face—direct excitation of ripples by wind and suppression of ripples by long waves

Ripples can be either generated by the wind or degenerated from long waves. The degeneration can be in the form of either wave breaking (Longuet-Higgins, 1969) or production of parasitic capillaries (Crapper, 1970). It is generally accepted that both kinds of rippling occur on the leeward face of long waves. In the present tank, as reported previously (Wu, 1968), the parasitic capillaries are produced at low wind velocities (U = 4.18, 6.92 m s^{-1}) in the surface tension governing regime of wind-wave interaction, and wave breaking takes place at high wind velocities (U = 9.60, 12.25 m s^{-1}) in the gravity governing regime of wind-wave interaction. Nontheless, it is seen in Fig. 2 that a considerable number of ripples exist on the windward face, especially the upper half, at all wind velocities. Moreover, as shown in Table 2 and discussed previously, the rms slope of ripples on the windward face is greater than that on the leeward face. In summary, not only is a significant portion of ripples on the windward face, but also the ripples on the windward face are actually much steeper than those on the leeward face. It appears then that most ripples, at least those on the windward face and consequently some on the leeward face, are generated directly by wind. It also indicates that the wind stress may vary along carrier waves with the stress being greater on the windward than on the leeward face.

It was suggested by Phillips and Banner (1974) that a nonlinear augmentation of the surface drift occurred near the crests of long waves as they moved across the surface. The ripples superimposed on their carrier waves therefore experience an augmented drift in these regions and consequently a further attenuation of their amplitudes. Experiments were also performed by Phillips and Banner with wind blowing over long, mechanically generated waves. They found a reduction in the energy density of a portion of the wave spectrum on the high-frequency side of the peak. A study under similar conditions was reported by Wu (1977b), who found that the rms surface slope with wind waves superimposing on preexisting long surface waves is smaller than without preexisting long waves. These experimental results indicate an overall suppression of small waves by long waves, but failed to provide evidence of the local suppression suggested by Phillips and Banner. The present results, which show the rms slope of ripples of the leeward face to be smaller than that on the windward face, however, provide more direct evidence of this localized suppression.

6. Concluding remarks

Previous measurements of this kind were either conducted at low wind velocities or attempted with the experimental technique limited to upwind and downwind looks. It is shown that the phenomena at high wind velocities are different from those at low wind velocities, and that the upwind and downwind looks do not provide description of ripples on the leeward and windward faces of the carrier waves. The present results obtained with conditional sampling over a wide range of wind velocities consist of the distributions and the slope statistics of ripples on various segments of the carrier-wave profile.

It is generally known and observed that there are more ripples on the leeward face of dominant wind waves than on the windward face. The present results, while confirming quantitatively such an observation, point out that although the leeward face seems rougher in appearance, the roughness is actually less steep than that on the windward face. The results that the rms slope is significant on the windward face indicate a direct generation of ripples by wind and may also indicate uneven distribution of wind stress along dominant waves. The fact that the rms slope is actually greater on the windward than on the leeward face appears to confirm the local suppression of ripples on the leeward face of long waves. The present results also provide more conclusive evidence on the steepening of ripples near the crests of long waves, and the flattening near the troughs.

Acknowledgment. The experiments were conducted earlier at Hydronautics, Inc. I am very grateful to the sponsorship of my previous and present work by the Fluid Dynamics Program, Office of Naval Research under Contract N00014-75-C-0285.

REFERENCES

Cox, C. S., 1958: Measurements of slopes of high-frequency wind waves. *J. Mar. Res.*, **16**, 199–225.

——, and Munk, W. H., 1956: Slopes of the sea surface deduced from photographs of sun glitter. *Bull. Scripps Inst. Oceanogr.*, **6**, No. 9, 401–488.

Crapper, G. D., 1970: Non-linear capillary waves generated by steep gravity waves. *J. Fluid Mech.*, **40**, 149–159.

Hasselmann, K., 1971: On the mass and momentum transfer between short gravity waves and large scale motions. *J. Fluid Mech.*, **50**, 189–205.

Jones, W. L., L. C. Schroeder, and J. L. Mitchell, 1977: Aircraft measurements of the microwave scattering signature of the ocean. *IEEE Trans. Antennas Propag.*, **AP-25**, 52–61.

Keller, W. C., and J. W. Wright, 1975: Microwave scattering and straining of wind-generated waves. *Radio Sci.*, **10**, 139–147.

Lee, P. H. Y., 1977: Doppler measurements of the effects of gravity waves on wind-generated ripples. *J. Fluid Mech.*, **81**, 225–240.

Long, S. R., and N. E. Huang, 1976: On the variation and growth of wave-slope spectra in the capillary-gravity range with increasing wind. *J. Fluid Mech.*, **77**, 209–228.

Longuet-Higgins, M. S., 1963: The generation of capillary waves by steep gravity waves. *J. Fluid Mech.*, **16**, 138–159.

——, 1969: A nonlinear mechanism for the generation of sea waves. *Proc. Roy. Soc. London*, **A311**, 371–389.

——, and R. W. Stewart, 1960: Changes in the form of short gravity waves on long waves and tidal currents. *J. Fluid Mech.*, **8**, 565–583.

Phillips, O. M., 1963: On the attenuation of long gravity waves by short breaking waves. *J. Fluid Mech.*, **16**, 321–332.

——, and M. L. Banner, 1974: Wave breaking in the presence of wind drift and swell. *J. Fluid Mech.*, **66**, 625–640.

Schooley, A. H., 1954: A simple optical method for measuring the statistical distribution of water surface slopes. *J. Opt. Soc. Amer.*, **44**, 37–40.

Wu, Jin, 1968: Laboratory studies of wind-wave interactions. *J. Fluid Mech.*, **34**, 91–112.

——, 1971: Slope and curvature distributions of wind-disturbed water surface. *J. Opt. Soc. Amer.*, **61**, 852–858.

——, 1972: Physical and dynamical scales for generation of wind waves. *J. Waterways, Harbor Coastal Eng. Div. ASCE*, **98**, WW2, 163–175.

——, 1973: Correlation of micro- and macroscopic structures of wind waves and differential roughening and smoothing of surface waves by wind. Hydronautics, Inc. Tech. Rep. 7211-6, 26 pp.

——, 1977a: Directional slope and curvature distributions of wind waves. *J. Fluid Mech.*, **79**, 463–480.

——, 1977b: Effects of long waves on wind boundary layer and on ripple slope statistics. *J. Geophys. Res.*, **82**, 1359–1362.

——, J. M. Lawrence, E. S. Tebay and M. P. Tulin, 1969: A multiple purpose optical instrument for studies of short steep water waves. *Rev. Sci. Instrum.*, **40**, 1209–1213.